*Proc. Natl. Acad. Sci. USA*
Vol. 74, No. 12, pp. 5524–5528, December 1977
Biochemistry

# Muscarinic acetylcholine receptors of the developing retina

(synapse formation/receptor localization/3-quinuclidinyl benzilate)

HIROYUKI SUGIYAMA, MATHEW P. DANIELS, AND MARSHALL NIRENBERG

Laboratory of Biochemical Genetics, National Heart, Lung, and Blood Institute, National Institutes of Health, Bethesda, Maryland 20014

*Contributed by Marshall Nirenberg, October 7, 1977*

ABSTRACT **Six- and 13-day chicken embryo retinas contain 10 and 320 fmol per mg of protein of specific binding sites for 3-[$^3$H]quinuclidinyl benzilate, a ligand of muscarinic acetylcholine receptors. Most of the receptors of 13-day embryo retina were found, by autoradiography, to be localized in two sharp bands within the inner synaptic layer of the retina. In the adult, the receptors were found almost exclusively in three bands in the inner synaptic layer of the retina. A possible mechanism for generating sets of stratified or columnar neurons and relating one set to another is proposed.**

The vertebrate retina provides a model system for synapse formation because synaptic circuits may be assembled with relatively few types of cells and because cultured neurons dissociated from retina form synapses in profusion *in vitro* (1, 2). Biochemical (3–7), histological (8, 9), and electrophysiological (10–13) evidence strongly suggests that acetylcholine (ACh) functions as a neurotransmitter in the retina. Developmental and histological studies of chicken retina acetylcholinesterase (EC 3.1.1.7 AChE) (8), ACh (14), choline acetyltransferase (EC 2.3.1.6) (2), and nicotinic ACh receptors (15, 16) have been reported.

In this report, the properties of muscarinic ACh receptors of chicken retina, the number of receptors, and their distribution within the retina during embryonic development are described.

## MATERIALS AND METHODS

**Homogenate Preparations.** Neural retinas of White Leghorn chicken embryos were homogenized in 50 mM sodium phosphate buffer, pH 7.4 (buffer A). In some experiments, homogenates were diluted several times with buffer A and centrifuged at 17,300 × *g* for 20 min at 3°. The pellet was suspended in buffer A (membrane fraction). All experiments were performed with freshly prepared homogenates or membranes.

**Binding Assay.** (3±)-Quinuclidinyl benzilate (QNB), a gift from Hoffman-La Roche, Inc., was labeled by catalytic $^3$H exchange and purified as described by Yamamura and Snyder (17); the specific activity was 8.4 Ci/mmol. 3(±)-[3-$^3$H] QNB used in some experiments was obtained from Amersham/Searle (13 Ci/mmol).

[$^3$H]QNB binding was measured by a modification of the method of Yamamura and Snyder (17). Homogenates were combined with [$^3$H]QNB in buffer A and incubated for various periods. Each 100- to 150-μl portion of the reaction mixture (usually containing 100–200 μg of protein) then was diluted into 5 ml of ice-cold buffer A, immediately filtered, and washed three times, each with 5 ml of buffer A. Binding kinetics were measured at 25° by using Whatman glass fiber GF/C filters. The concentration of (±)-[$^3$H]QNB in the reaction mixture was 0.5–1.0 nM. When the effects of competing ligands were tested, homogenates were incubated with desired concentrations of ligands for 5–10 min at 25° and then mixed with [$^3$H]QNB solution containing the same concentrations of the ligands. Equilibrium studies were performed at 4° with Millipore HAWP filters or, in some cases, GF/C filters (results were essentially the same). For the determination of nonspecific binding, homogenates were incubated with 0.4–10 μM atropine sulfate for 10 min in ice and then mixed with [$^3$H]QNB solution containing the same concentration of atropine. The number of [$^3$H]QNB binding sites was determined by Scatchard analysis in some experiments but more often was determined at one saturating concentration of (±)-[$^3$H]QNB (6–10 nM).

**[$^3$H]QNB Autoradiography.** Neural retinas were dissected in cold Dulbecco's phosphate-buffered saline with $Ca^{2+}$ and $Mg^{2+}$ (PBS). Pieces of retina from 13-day embryos or adult chickens were incubated for 90 min in 5 ml of PBS containing 4 or 2 nM (±)-[$^3$H]QNB (13 Ci/mmol), respectively, and then washed eight times, each with 5 ml of PBS. In control experiments, pieces of retina were preincubated in 5 ml of PBS containing 0.4 μM atropine sulfate for 10 min, followed by incubation in 5 ml of [$^3$H]QNB solution in PBS containing 0.4 μM atropine sulfate for 90 min. The tissue then was washed twice with 5 ml of PBS containing 0.4 μM atropine sulfate and six times with 5 ml of PBS. Samples were kept in an ice bath at each step. Both experimental and control retinas were washed for 25 min (all washes). Retinas then were sandwiched between two pieces of mouse liver and frozen quickly in liquid Freon cooled in liquid nitrogen. Frozen pieces were sectioned (12 μm thick) and thaw-mounted onto glass slides coated with Kodak NTB-2 nuclear emulsion. To minimize diffusion of [$^3$H]QNB, mounted sections were immediately dried under a stream of nitrogen gas. Slides were stored in the dark at 4° with a desiccant. Autoradiographs were developed, fixed, and then immersed in 2.5% glutaraldehyde in 0.1 M phosphate buffer, pH 7.0, for 1 hr at room temperature. Some slides were stained with 0.02% toluidine blue for 5 min at room temperature.

**Retina Cell Cultures.** Cells were prepared from 8-day embryos and cultured in rotating petri dishes as described (1) with minor modifications: 1.5 × $10^7$ cells in 3 ml of medium (95% Eagle's basal medium with Earle's salts and 5% fetal bovine serum) were cultured in a bacterial petri dish (35 mm; Falcon no. 1008) placed on a rotary shaker with an excursion of 2.6 cm (75–80 rpm) in a 37° incubator in a humidified atmosphere of 5% $CO_2$/95% air. Half of the medium was replaced each day.

The costs of publication of this article were defrayed in part by the payment of page charges. This article must therefore be hereby marked "*advertisement*" in accordance with 18 U. S. C. §1734 solely to indicate this fact.

Abbreviations: ACh, acetylcholine; AChE, acetylcholinesterase; QNB, 3-quinuclidinyl benzilate; PBS, phosphate-buffered saline with $Ca^{2+}$ and $Mg^{2+}$.

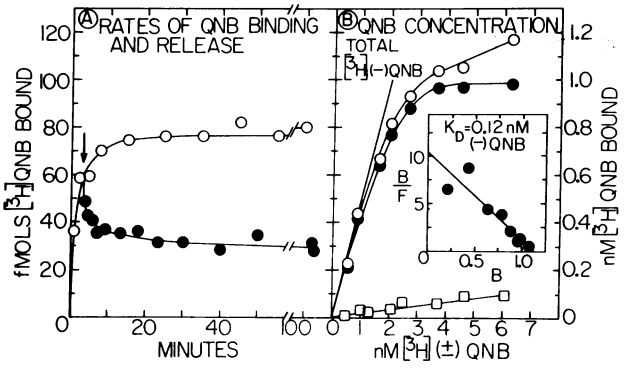


FIG. 1. QNB binding to receptors in homogenates of 13-day chicken embryo retina. (*A*) Kinetics of QNB binding to and release from sites on membrane preparations at 25°. The ordinate represents specific binding of [$^3$H]QNB per 0.273 mg of protein (0.15 and 3.0 ml reaction mixtures for on and off reactions, respectively). The initial concentration of (±)-[$^3$H]QNB was 2.0 nM. For the release kinetics experiment, the reaction mixture was incubated for 3 min and then diluted with 19 volumes of buffer A containing 0.4 μM atropine. Fifty-seven min after the first dilution, the reaction mixture was again diluted 20-fold with buffer A with 0.4 μM atropine. No release of QNB was observed during further incubation (not shown). (*B*) QNB concentration curve and Scatchard plot (*Inset*). Specific binding (●) is the difference between total binding (○) and nonspecific binding (□) in the presence of 0.4 μM atropine. Each point represents the mean of triplicate values. B and F correspond to concentrations (nM) of specifically bound QNB and free (−)-QNB, respectively. The line without points represents the concentration of active isomer (−)-QNB added. The concentration of protein in the reaction mixture was 2.86 mg/ml. Tubes were incubated at 4° for 100 min.

## RESULTS

**Receptor Properties.** The rates of [$^3$H]QNB binding to and release from receptors in homogenates of 13-day chicken embryo retina are shown in Fig. 1*A*. [$^3$H]QNB bound rapidly to retina membranes; in the presence of 2 nM (±)-[$^3$H]QNB, half maximal binding was achieved in 2 min and maximal binding, in approximately 15 min. Some, but not all, of the reactions are reversible. The addition of 0.38 μM atropine and dilution of reaction mixtures 20-fold resulted in the dissociation of approximately 50% of the [$^3$H]QNB–receptor complex. QNB association and dissociation reactions both exhibited biphiasic kinetics with fast and slow association reactions and dissociation reactions. The kinetics will be discussed elsewhere; however, the rate constants (*k*) for fast and slow QNB association reactions were estimated, by assuming bimolecular irreversible reactions as a first approximation, to be $2.7 \times 10^8$ $M^{-1}$ $min^{-1}$ and $1.4 \times 10^8$ $M^{-1}$ $min^{-1}$, respectively. Both fast and slow QNB–receptor dissociation reactions were first-order reactions with rate constants of 1.2 $min^{-1}$ and 0.041 $min^{-1}$, respectively.

The relationship between [$^3$H]QNB concentration and binding to receptors in retina is shown in Fig. 1*B*. The binding of the pharmacologically active isomer, (−)-[$^3$H]QNB, to retina receptors is a saturable process. In the presence of 0.4 μM atropine, relatively little nonspecific [$^3$H]QNB binding was found with homogenates prepared from 13-day chicken embryo retina; however, nonspecific [$^3$H]QNB binding was markedly increased when homogenates are prepared from >15-day chicken embryo retina or posthatched retina. The dissociation constant ($K_D$) determined by Scatchard analysis (Fig. 1*B* and *inset*) was 0.12 nM (−)-[$^3$H]QNB. However, we consistently observed higher apparent dissociation constants (~0.4 nM) with homogenates from retina of chickens 2 weeks after hatching and of adult chickens. The calculated concentration of specific QNB binding sites in 13-day chicken embryo retina is 325

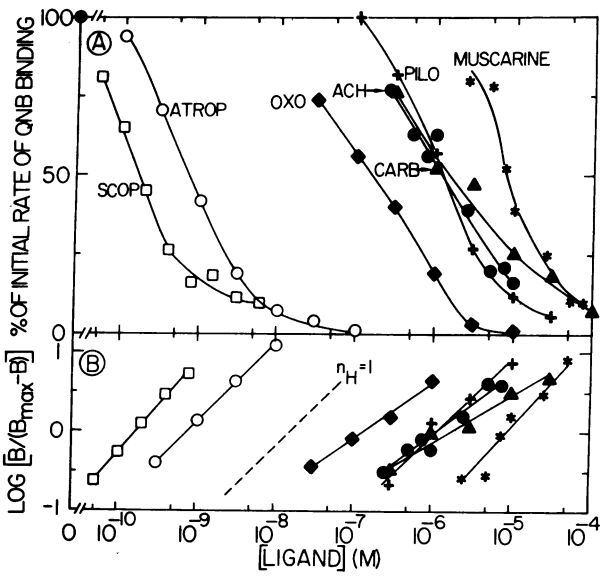


FIG. 2. (*A*) Inhibition of [$^3$H]QNB binding by various compounds. (*B*) Hill plot. Thirteen-day embryo retinas were used. Whole homogenates and membrane fractions were used and no significant difference was noted. The final concentration of (±)-[$^3$H]QNB was 0.5 nM (1.0 nM in some experiments). Protein concentrations in reaction mixtures were 0.5–2.6 mg/ml. Receptor concentrations were 0.1–1.0 nM. Initial rates of binding (usually 0 to 3–4 min) were fitted to a model of bimolecular irreversible reaction mechanism, and the bimolecular association rate constant was calculated. The apparent rate constant in the presence of protecting drugs was expressed as the percentage of the control value in *A*. Hill plots were obtained by assuming that the percentage decrease of [$^3$H]QNB binding rate represents the percentage of the receptor sites occupied by unlabeled ligands which corresponds to $B/B_{max}$. When ACh was tested the homogenate was preincubated with 3 μM eserine for 30 min at 25° before addition of ACh. Symbols: □, scopolamine; ○, atropine sulfate; ♦, oxotremorine; ●, AChCl; ▲, carbamylcholine chloride; +, pilocarpine; *, muscarine.

fmol/mg of protein and each retina contained 818 fmol per retina ($4.9 \times 10^{11}$ sites per retina) of specific QNB binding sites. The apparent Hill coefficient is 1.0 (plot not shown), which suggests that QNB binds to independent, noninteracting receptors. Although only one population of QNB binding sites was detected by Scatchard analysis, kinetics of the QNB binding to and release from receptors show that [$^3$H]QNB–receptor complexes are heterogeneous.

The effects of different concentrations of unlabeled ligands known to activate or inhibit muscarinic ACh receptors on the initial rate of [$^3$H]QNB binding to receptors in homogenates prepared from 13 day chick embryo retina are shown in Fig. 2*A*. [$^3$H]QNB binding was markedly decreased in the presence of antagonists of muscarinic ACh receptors such as scopolamine or atropine or receptor activators such as oxotremorine, ACh, carbamylcholine, pilocarpine, or muscarine at expected physiological concentrations. [$^3$H]QNB binding was not affected by prior incubation of homogenates with 10 nM α-bungarotoxin for 3 hr at 25° (not shown). Thus, the specificity of QNB binding sites for ligands closely resembles that of muscarinic ACh receptors.

As shown in Fig. 2*B*, the apparent Hill coefficients of activators of the muscarinic ACh receptor such as oxytremorine, ACh, and carbamylcholine were 0.6 to 0.8, whereas those of receptor antagonists were approximately 1. These results agree well with those of Birdsall *et al.* (18). The apparent Hill coefficients of pilocarpine and muscarine were approximately 1. Pilocarpine has been shown to be both an activator and an an-

Table 1. Apparent dissociation constants and Hill coefficients of ligands for muscarinic acetylcholine receptors of 13 day chick embryo retina

| Ligands | | App $K_D$,* nM | h |
|---|---|---|---|
| Antagonists | | | |
| QNB | 4° | 0.12 | 1.0 |
| | 25° | 0.44 | 1.0 |
| | | 0.29† | — |
| Atropine | | 0.69 | 1.0 |
| Scopolamine | | 0.17 | 1.1 |
| Activators | | | |
| Oxotremorine | | 130 | 0.7 |
| Acetylcholine | | 1,100 | 0.8 |
| Carbamylcholine | | 1,700 | 0.6 |
| Muscarine | | 8,700 | 1.1 |
| Pilocarpine | | 1,100 | 1.0 |
| Local anesthetics | | | |
| Dibucaine | | 30,000 | 1.0 |
| Tetracaine | | 21,000 | 1.1 |

* Values at 25° except otherwise specified. The $K_D$ values for QNB were obtained by determining the binding of [$^3$H]QNB at equilibrium. The $K_{app}$ values for the other antagonists and activators represent the concentrations that result in 50% inhibition of the initial rate of [$^3$H]QNB binding; values were not corrected for h < 1. The $K_{app}$ values for local anesthetics are estimated from experiments where the retina homogenate with or without different concentrations of a local anesthetic were incubated for 60 min at 25° in the absence of [$^3$H]QNB, then 0.50 nM (±)-[$^3$H]QNB was added and the reaction mixtures were incubated for an additional 5 min.

† 0.29 and 4.4 nM (−)-QNB are the dissociation constant values determined from rate constants for slow and fast association and dissociation reactions, respectively.

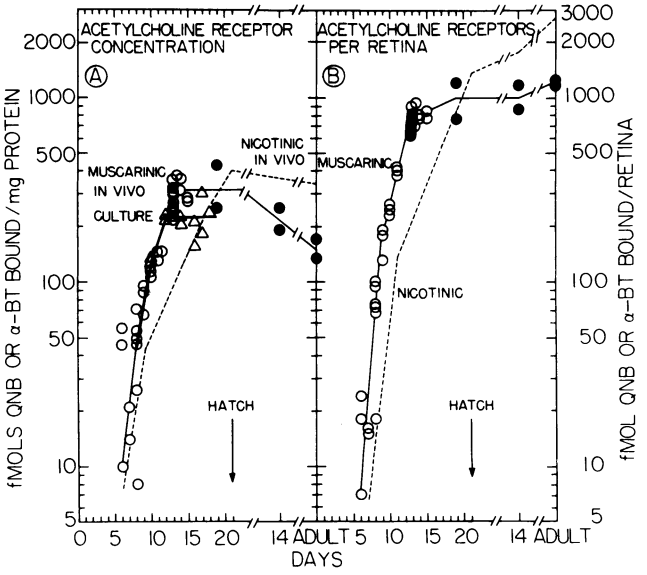


FIG. 3. The accumulation of QNB binding sites in chicken embryo retina as a function of development age. The number of specific sites per mg protein (*A*) or per retina (*B*) is shown. For comparison, α-bungarotoxin (α-BT) binding to nicotinic ACh receptors (16) is shown (broken lines). Circles, intact retina *in vivo*; triangles, cultured cells dissociated from 8-day chicken embryo retina. Filled circles are values obtained by Scatchard analysis. Open symbols represent the specific binding obtained at 6–10 nM (±)-[$^3$H]QNB. Tubes were incubated at 4° for 60 min. In some cases, the retina dissection was not complete; the amount of protein per retina then was estimated from the published values (19). Each point represents the mean of at least three determinations.

tagonist of the muscarinic ACh receptor; although muscarine is an activator of the muscarinic ACh receptor in other organisms, the apparent Hill coefficient with chicken embryo retina receptors resembles that of a receptor antagonist. The apparent Hill coefficients of <1 observed with oxytremorine, ACh, and carbamylcholine can be interpreted in various ways such as negative cooperativity, heterogeneity of binding sites, or desensitization of the ACh receptor. The demonstration by W. Klein in this laboratory that heterogeneity of muscarinic ACh receptors can be detected by kinetic studies was confirmed.

**Muscarinic ACh Receptors during Embryonic Development.** The concentration and number of muscarinic ACh receptors in chicken embryo retina are shown in Fig. 3 *A* and *B*, respectively, as a function of developmental age. Values reported for nicotinic ACh receptors (16) also are shown for comparison. Muscarinic ACh receptors were detected in 5.5-day embryo retina, but the concentration was relatively low (10 fmol/mg of protein). Between the 6th and 14th days of embryonic development, the concentration of specific QNB binding sites increased 30-fold. In the 5.5- to 9-day chicken embryo retina, specific QNB binding sites accumulated exponentially with a doubling time of approximately 26 hr; in 9- to 14-day embryo retina, the doubling time was approximately 60 hr. The maximal concentration of QNB binding sites (320 fmol/mg of protein) was attained in the retina of the 13- to 14-day embryo. No further change was detected during later embryonic development; however, receptor concentrations were lower in retina 2 weeks after hatching and in adult retina. Although the concentration of receptors decreased after hatching, the number of receptors per retina increased slightly after hatching (Fig. 3*B*). The adult chick retina contained 1200 fmol of specific QNB binding sites per retina ($7.2 \times 10^{11}$ sites per retina).

These results show that genes for muscarinic ACh receptors are expressed early in the development of the retina and suggest that some neurons synthesize muscarinic ACh receptors but not neuroblasts as reported for nicotinic ACh receptors (16). The number of muscarinic and nicotinic ACh receptors increase more than 30-fold and the receptors accumulate at similar rates between the sixth and ninth days in embryos. The maximal concentration of muscarinic ACh receptors is attained in the retina of the 13-day embryo, whereas nicotinic ACh receptors continue to increase until hatching. The concentration of specific QNB binding sites in retina of the 6- to 13-day embryo is 2- to 3-fold higher than the concentration of α-bungarotoxin binding sites; however, this ratio is reversed in the adult retina. Thus, the ratio of muscarinic to nicotinic ACh receptor changes markedly during retina development.

Cells dissociated from 8-day chicken embryo retina were cultured for various times in rotating petri dishes. At various times, homogenates were assayed for specific binding of [$^3$H]QNB (Fig. 3*A*). The concentration of QNB binding sites increased from 50 fmol of specific QNB binding sites per mg of protein in retina of the 8-day embryo to 225 fmol/mg of protein after 4 days of culture. Thus, the accumulation of muscarinic ACh receptors in cultured retina cells resembled that in the intact retina.

**Receptor Distribution in Retina.** The distribution of [$^3$H]QNB binding sites in intact 13-day chicken embryo retina and in adult retina is shown in Fig. 4. In 13-day embryo retina, most of the silver grains were localized in two narrow bands within the inner synaptic layer of the retina (also termed "inner plexiform layer") (Fig. 4 *A* and *B*). In adult retina (Fig. 4 *C* and

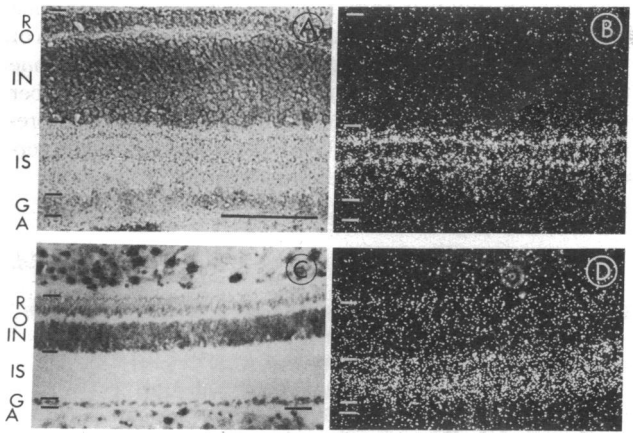


FIG. 4. Autoradiography of sections of chicken retina incubated with [$^3$H]QNB in the absence of atropine. (*A*) Phase-contrast view and (*B*) dark-field view of stained section of 13-day embryo retina exposed for 390 days. (*C*) Phase-contrast view and (*D*) dark-field view of stained section of adult chicken retina exposed for 173 days. (Bars represent 100 $\mu$m.) Lines at the left of each photograph represent the boundaries of layers: R, photoreceptor layer; O, outer synaptic layer; IN, inner nuclear layer; IS, inner synaptic layer; G, ganglion cell layer; A, ganglion axon layer.

*D*), two or three bands of silver grains could be seen within the inner synaptic layer of the retina.

Histograms relating the density of silver grains on autoradiographs that had been exposed for shorter times with grain location over the retina are shown in Fig. 5. Two sharply defined bands of silver grains of equal density can be seen within the inner synaptic layer of 13-day embryo retina. Fewer silver grains were associated with the lower portion of the inner nuclear layer (cell bodies of amacrine and bipolar neurons and Muller cells) and with ganglion neuron soma and axons but were not associated with other regions of the retina. The average number of silver grains over the entire retina incubated in the absence or presence of 0.4 $\mu$M atropine (nonspecific [$^3$H]QNB binding) was 3.83 and 0.87 grain per 100 $\mu$m$^2$, respectively.

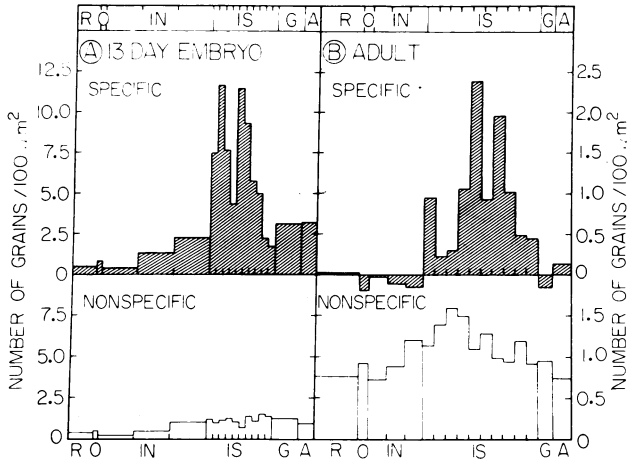


FIG. 5. Histograms showing the grain distribution in [$^3$H]QNB autoradiographs of sections of 13-day chicken (*A*) or adult chicken (*B*) retina. Sections of retina of both ages, treated for both total binding and nonspecific binding, were subjected to autoradiography for 65 days. Grains were counted at ×600 magnification by using a camera lucida. Specific binding was obtained by subtracting nonspecific from total binding. Number of grains counted were: 543 and 220 for total and nonspecific binding, respectively, for 13-day embryo retina; 1592 and 847 for total and nonspecific binding, respectively, for adult retina. Abbreviations are as in Fig. 4.

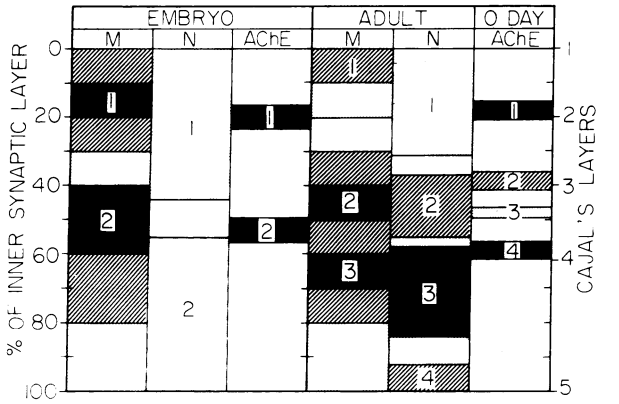


FIG. 6. Schematic representation of the relative distributions and concentrations of muscarinic (M) and nicotinic (N) ACh receptors (16) and AChE activity (8) in the inner synaptic layer of chick retina. M and N are from 13-day embryo or adult retinas; AChE is from 12-day embryo and newly hatched chicken retinas. Open, stippled, hatched, and filled areas represent relative ACh receptor concentrations or AChE activity in increasing order. Numbers refer to peak positions. The top and the bottom of the figure (0 and 100%) correspond to the inner nuclear and ganglion neuron boundaries of inner synaptic layer, respectively. Cajal's layers for chicken retina are from plates 4 and 5 of ref. 20.

Thus, specific QNB binding accounted for 77% of total QNB binding. In the adult retina (Fig. 5*B*), three bands of specific QNB binding sites were localized in the inner synaptic layer of the retina. Few, if any, specific binding sites for QNB were detected elsewhere in the retina; thus, muscarinic ACh receptors are localized to a greater extent in the adult retina than in the 13-day embryo retina. In other sections, the first band of specific QNB binding sites near the inner nuclear layer overlapped the first and second fractions of the inner synaptic layer and the demarcation between the second and third bands was less distinct than that shown. The average number of silver grains over the entire retina in the absence or presence of 0.4 $\mu$M atropine was 1.39 and 0.96 grain per 100 $\mu$m$^2$, respectively. Specific [$^3$H]QNB binding was 31% of total QNB binding, in accord with ligand binding results. Adult retina was incubated with 2 rather than 4 nM [$^3$H]QNB to decrease nonspecific [$^3$H]QNB binding; however, the grain density was somewhat lower than expected.

These results show that muscarinic ACh receptors are localized in the inner synaptic layer of the retina and suggest that the receptors are present in some amacrine and ganglion neurons but not in other cell types in the retina.

## DISCUSSION

The distribution of muscarinic ACh receptors within the inner synaptic layer of chicken embryo and adult retina is compared with previously reported distributions of nicotinic ACh receptors (16) and AChE activity (8) in Fig. 6. Muscarinic and nicotinic ACh receptors and AChE activity are localized in bands within the inner plexiform layer of chick retina. In the embryo, two bands, each with high concentrations of muscarinic ACh receptors and high AChE activity, can be seen; nicotinic ACh receptors are distributed diffusely in two broad bands throughout most of the inner synaptic layer. After hatching, the inner synaptic layer of the retina contains three muscarinic ACh receptor bands, four nicotinic ACh receptor bands (16), and four bands with high AChE activity (8). Nicotinic ACh receptors are present in the outer synaptic layer (16), but not muscarinic receptors. Most, but not all, of the ACh receptor bands are associated with AChE bands. The bands appear in

an ordered sequence during development, with respect to temporal and positional relationships. The maximal concentrations of muscarinic and nicotinic ACh receptors are attained on the 13th and 21st days of embryonic development. Thus, most of the synapses mediated by muscarinic ACh receptors probably are formed at an earlier developmental stage in retina than those mediated by nicotinic ACh receptors. Vogel *et al.* (21) have shown that nicotinic ACh receptors are localized at sites of synapses in chicken retina. The localized bands of muscarinic ACh receptors within the inner synaptic layer and the apparent absence of the receptors from cell bodies and axons of ganglion neurons in adult retina raise the possibility that muscarinic receptors also may be localized at certain synapses. Further work is needed to resolve this question.

Bipolar neurons and photoreceptors of retina form double or triple synapses (ribbon synapses) wherein one cell transmits information across one synapse simultaneously to two or three neurons. ACh probably is the transmitter at some double synapses of bipolar neurons because localized nicotinic ACh receptors have been found on the processes of one or both postsynaptic cells (21). Because three species of ACh receptor—muscarinic excitatory, muscarinic inhibitory, and nicotinic—are widely distributed in the nervous system, ACh released at one synapse may excite and/or inhibit the recipient neurons, depending on the species of ACh receptor that are present.

The inner synaptic layer is composed predominantly of neurites of amacrine, bipolar and ganglion neurons, and synaptic connections with processes of ganglion, amacrine, or bipolar neurons. Five layers can be distinguished by phase-contrast microscopy but not by transmission electron microscopy within the inner synaptic layer. However, Dubin (22) has shown that three classes of synapses that can be identified by ultrastructural features are stratified in different ways in the inner synaptic layer of pigeon retina; stratification was not detected in the retina of other organisms examined.

Eleven layers can be distinguished within the inner synaptic layer of chick retina on the basis of ACh receptor concentrations and AChE activity. Three additional layers rich in catecholamines have been identified in the inner synaptic layer of chicken retina (5), and four or five glutamic acid decarboxylase bands have been detected in rat retina (23). These results show that neurites of one type sort out from those of other types. A neuron that forms synaptic connections with two or more neurons is, in effect, a polyvalent crosslinking agent. Thus, neighboring neurons that form synapses with two or more cells of the same type, at the same stage of development, become linked to one another and sort out from other sets of neurons. Since a single neuron may both send and receive information across synapses and may form multiple kinds of synapses, such neurons may link sets of neurons that form different types of synapses. The extent of sorting out and the relationship of one class of neurons to another may be determined by the number and kinds of synapses formed by each class of neurons (both pre- and postsynaptic connections), the sequence of synapse formation, and the initial spatial relationships of the neurons.

We thank Linda Lee for excellent assistance.

1. Vogel, Z., Daniels, M. P. & Nirenberg, M. (1976) *Proc. Natl Acad. Sci. USA* **73**, 2370–2374.
2. Puro, D. G. DeMello, F. G. & Nirenberg, M. (1977) *Proc. Natl. Acad. Sci. USA* **74**, 4977–4981.
3. Graham, L. T., Jr. (1974) in *The Eye*, eds. Davson, H. & Graham, L. T., Jr. (Academic Press, New York), Vol. 6, pp. 283–342.
4. Neal, M. J. (1976) in *Transmitters in the Visual Processes*, ed. Bonting, S. L. (Pergamon Press, New York), pp. 127–143.
5. Ehinger, B. (1976) in *Transmitters in the Visual Processes*, ed. Bonting, S. L. (Pergamon Press, New York), pp. 145–163.
6. Ross, C. D. & McDougal, D. B., Jr. (1976) *J. Neurochem.* **26**, 521–526.
7. Lam, D. M. K. (1976) *Cold Spring Harbor Symp. Quant. Biol.* **40**, 571–579.
8. Shen, S. C., Greenfield, P. & Boell, E. J. (1956) *J. Comp. Neurol.* **106**, 433–461.
9. Spira, A. W. (1974) *J. Histochem. Cytochem.* **22**, 868–880.
10. Masland, R. H. & Ames, A., III (1976) *J. Neurophysiol.* **39**, 1220–1235.
11. Straschill, M. & Perwein, J. (1973) *Pflügers Arch.* **339**, 289–298.
12. Vivas, I. A. & Drujan, B. D. (1977) *6th Meeting International Soc. Neurochem.*, p. 149 (Abstract).
13. Noell, W. K. & Lasansky, A. (1959) *Fed. Proc.* **18**, 115.
14. Lindeman, V. F. (1947) *Am. J. Physiol.* **148**, 40–44.
15. Wang, G. K. & Schmidt, J. (1976) *Brain Res.* **114**, 524–529.
16. Vogel, Z. & Nirenberg, M. (1976) *Proc. Natl Acad. Sci. USA* **73**, 1806–1810.
17. Yamamura, H. I. & Snyder, S. H. (1974) *Proc. Natl. Acad. Sci. USA* **71**, 1725–1729.
18. Birdsall, N. J. M., Burgen, A. S. V., Hiley, C. R. & Hulme, E. C. (1976) *J. Supramol. Struct.* **4**, 367–371.
19. DeMello, F. G., Bachrach, U. & Nirenberg, M. (1976) *J. Neurochem.* **27**, 847–851.
20. Ramon y Cajal, S. (1972) *The Structure of the Retina*, translated by Thorpe, S. A. & Glickstein, M. (Charles C Thomas, Springfield, IL).
21. Vogel, Z., Maloney, G. J., Ling, A. & Daniels, M. P. (1977) *Proc. Natl. Acad. Sci. USA* **74**, 3268–3272.
22. Dubin, M. W. (1970) *J. Comp. Neurol.* **140**, 479–505.
23. Barber, R. & Saito, K. (1976) in *GABA in Nervous System Function*, eds. Roberts, E., Chase, T. N. & Tower, D. B. (Raven Press, New York), pp. 113–132.